International Journal of Bifurcation and Chaos, Vol. 35, No. 14 (2025) 2540004 (13 pages)

DOI: 10.1142/S0218127425400048

Multistability in a 3D Circulant Chaotic Flow: The Circulant Symmetry of Coexisting Dynamics

Karthikeyan Rajagopal
Center for Research, SRM Easwari Engineering College, Chennai 600089, India
Center for Cognitive Science, Trichy SRM Medical College Hospital and Research Center, Trichy 621105, India
rkarthiekeyan@gmail.com

Fahimeh Nazarimehr *,‡ and Sajad Jafari *,†,§
**Department of Biomedical Engineering, Amirkabir University of Technology (Tehran Polytechnic), Tehran 1591634311, Iran*
†Health Technology Research Institute, Amirkabir University of Technology (Tehran Polytechnic), Tehran 1591634311, Iran
‡f_nazarimehr@aut.ac.ir; fahimenazarimehr@yahoo.com
§sajadjafari@aut.ac.ir

Julien C. Sprott
Department of Physics, University of Wisconsin–Madison, Madison, WI 53706, USA
csprott@wisc.edu

Received May 21, 2025; Accepted July 27, 2025; Published October 16, 2025

In this paper, a novel chaotic flow exhibiting circulant symmetry is modeled and analyzed. The chaotic flow's dynamical behavior is thoroughly investigated, revealing that it is dissipative over the studied parameter values. A basic equilibrium analysis shows that four of the system's equilibrium points are stable. Notably, the system exhibits two distinct sets of three coexisting chaotic attractors, each set displaying circulant symmetry. To the best of our knowledge, such a system has not been previously reported in the literature. Bifurcation analysis with respect to all three system parameters confirms the rich dynamical behavior, supported by corresponding Lyapunov exponent spectra. The basins of attraction reveal rare V-shaped boundaries, adding to the system's uniqueness. Furthermore, the circulant symmetry is clearly reflected in the basins of attraction of the coexisting attractors.

Keywords: Circulant symmetry; chaos; dissipative; multistability.

‡Author for correspondence

1. Introduction

Chaos theory is a fascinating field of research that is a cornerstone of nonlinear dynamics; it provides an insight into the understanding of deterministic yet unpredictable behaviors of real-world systems [Bob, 2007; Sprott, 2010; Danca, 2024; Pan *et al.*, 2025]. The main feature of chaotic systems is sensitive dependence on initial conditions, which makes them a proper choice for applications in diverse fields such as secure communication [Banerjee, 2010; Almatroud *et al.*, 2024], cryptography [Lawnik *et al.*, 2022; Tutueva *et al.*, 2022], and biological modeling [Panahi *et al.*, 2019; Wang *et al.*, 2024; Zhang *et al.*, 2025]. For many years, there was an idea that chaotic attractors are related to saddle equilibria [Rössler, 1976], until some counterexamples were proposed showing chaos without any equilibrium points [Wei, 2011] or with one stable equilibrium [Wang & Chen, 2012]. After that, the idea was broken, and many chaotic systems with various equilibrium points were proposed [Danca, 2017]. Various studies have been done to untangle the mystery of the generation of chaos in nonlinear dynamical systems [Xu *et al.*, 2020; Shukur *et al.*, 2025]. Chaotic dynamics of memristive neurons have attracted a lot of attention [Xu *et al.*, 2024a; Xu *et al.*, 2024b].

Despite many trials, there are many unknown mysteries in studying chaotic flows. Some systems have features like multistability or adjustable dynamics, while many have complex topologies that make them challenging to work with [Nazarimehr & Sprott, 2020; Khan *et al.*, 2025; Raza *et al.*, 2025]. Furthermore, organized systems, such as those with symmetry, are yet largely unexplored. One interesting type of these systems is circulant systems, which have cyclic permutation characteristics and rotational symmetry [Sprott, 2010]. They are especially attractive for new technologies because of their intrinsic symmetry, which helps streamline theoretical analysis and real-world applications.

Symmetry plays a crucial role in understanding the behavior of dynamical systems. Many chaotic systems exhibit reflectional symmetry [Kyurkchiev *et al.*, 2024]. More recent works have explored chaotic systems with permutation symmetry, where variables can be cyclically interchanged without altering the system's dynamics [Rajagopal *et al.*, 2019; Panahi *et al.*, 2021]. Notably, several algebraically simple chaotic flows with symmetry properties have been introduced [Li & Sprott, 2021; Li *et al.*, 2022]. However, few studies have focused on systems with circulant symmetry, where each variable is a cyclic permutation of the others in the governing equations [Sprott, 2010].

In this study, we present a new circulant chaotic system with cubic nonlinearities intended to show coexisting attractors and rich dynamical behavior. The system's nonlinear terms allow for intricate stretching and folding dynamics that are necessary for chaos, while its circulant structure guarantees rotational symmetry. We illustrate a variety of phenomena, such as multistability, period-doubling pathways to chaos, and crisis-induced transitions, by altering important constants. Our research advances our theoretical knowledge of circulant systems while simultaneously demonstrating its potential for real-world uses in secure communication and random number generation.

This is how the rest of the paper is structured. The mathematical description of the suggested system is shown in Sec. 2, focusing on its nonlinear structure and circulant symmetry. The dynamical behavior of the system, including phase portraits, bifurcation diagrams, and Lyapunov exponents, is examined in Sec. 3. In order to provide more light on the chaotic characteristics of the system, Sec. 3.4 examines the basin of attraction. A review of the main conclusions and possible future directions is provided in Sec. 4, which brings the paper to a close.

2. Mathematical Formulation

Here, we propose a circulant chaotic flow with cubic nonlinearities, designed to exhibit coexisting attractors. Circulant systems are defined by rotational symmetry in their governing equations, ensuring cyclic permutation of variables [Sprott, 2010]. Our system adheres to the general form

$$\begin{aligned} \dot{x} &= g(x, y, z), \\ \dot{y} &= g(y, z, x), \\ \dot{z} &= g(z, x, y), \end{aligned} \tag{1}$$

where $g(\cdot)$ is a nonlinear function preserving circulant symmetry. Through an exhaustive computational search for chaotic dynamics, we derive the following system:

$$\begin{aligned} \dot{x} &= ax + b(y + z)yz + cyz, \\ \dot{y} &= ay + b(z + x)zx + czx, \\ \dot{z} &= az + b(x + y)xy + cxy. \end{aligned} \tag{2}$$

Table 1. Equilibrium points and their stabilities of system (2).

#	Equilibrium Points			Eigen Values			Stability
	x	y	z	λ_1	λ_2	λ_3	
1	0.0000	0.0000	0.0000	-0.0556	-0.0556	-0.0556	Stable
2	-0.1516	-0.4819	-0.4819	$-0.0643 + 0.2108i$	$-0.0643 - 0.2108i$	-0.0381	Stable
3	-0.4819	-0.1516	-0.4819	$-0.0643 + 0.2108i$	$-0.0643 - 0.2108i$	-0.0381	Stable
4	-0.4819	-0.4819	-0.1516	$-0.0643 + 0.2108i$	$-0.0643 - 0.2108i$	-0.0381	Stable
5	0.2131	0.2131	-1.1654	-0.3594	$0.0964 + 0.3785i$	$0.0964 - 0.3785i$	Unstable
6	-0.2841	-0.2841	-0.6273	0.0671	$-0.1169 + 0.0953i$	$-0.1169 - 0.0953i$	Unstable
7	0.0529	0.0529	-0.0557	0.0571	-0.1141	-0.1097	Unstable
8	-0.4363	-0.4363	-0.4363	-0.3252	0.0793	0.0793	Unstable
9	-0.0637	-0.0637	-0.0637	-0.1071	-0.1071	0.0475	Unstable
10	-0.2841	-0.6273	-0.2841	0.0671	$-0.1169 + 0.0953i$	$-0.1169 - 0.0953i$	Unstable
11	-0.6273	-0.2841	-0.2841	$-0.1169 + 0.0953i$	$-0.1169 - 0.0953i$	0.0671	Unstable
12	0.05297	-0.0557	0.0529	0.0571	-0.1141	-0.1097	Unstable
13	-0.0557	0.0529	0.0529	-0.1097	0.0571	-0.1141	Unstable
14	0.2131	-1.1654	0.2131	-0.3594	$0.0964 + 0.3785i$	$0.0964 - 0.3785i$	Unstable
15	-1.1654	0.2131	0.2131	$0.0964 + 0.3785i$	$0.0964 - 0.3785i$	-0.3594	Unstable

Each equation is a cyclic permutation of variables. The cubic nonlinearities, such as $b(y+z)yz$ and cyz, introduce strong nonlinear interactions critical for chaos. The system can show chaotic dynamics where the parameters are $a = -\frac{1}{18}$, $b = -1$, $c = -1$. The divergence of the vector field is $3a = -\frac{1}{6}$ (for $a = -\frac{1}{18}$), ensuring volume contraction in phase space — a prerequisite for chaos. Parameter a governs linear damping, while b and c control nonlinear coupling, with b amplifying cross-terms like $(y+z)yz$. Cubic terms enable complex stretching/folding dynamics, while the linear term ax stabilizes trajectories since the a's sign is negative.

As the most fundamental feature of a chaotic flow, the equilibrium points of the system are investigated. These points are obtained by solving the following system of equations:

$$\begin{aligned} \dot{x} &= ax + b(y+z)yz + cyz = 0, \\ \dot{y} &= ay + b(z+x)zx + czx = 0, \\ \dot{z} &= az + b(x+y)xy + cxy = 0. \end{aligned} \tag{3}$$

Numerical methods implemented in MATLAB were utilized to calculate equilibrium points as presented in Table 1. To investigate the stability of each fixed point, the system's Jacobian matrix is calculated as follows:

$$\mathbf{J} = \begin{bmatrix} a & 2byz + bz^2 + cz & by^2 + 2byz + cy \\ bz^2 + 2bxz + cz & a & 2bzx + bx^2 + cx \\ 2bxy + by^2 + cy & bx^2 + 2bxy + cx & a \end{bmatrix}. \tag{4}$$

Then, for each equilibrium point, the characteristic equation is constructed as

$$\det(\lambda \mathbf{I} - \mathbf{J}|_{\mathrm{FP}}) = 0,$$

where FP denotes the fixed point. The eigenvalues corresponding to each equilibrium point are presented in Table 1. The eigenvalue analysis reveals that the first four equilibrium points are stable, as the real components of all eigenvalues are negative. The remaining equilibrium points are unstable, with at least one eigenvalue containing a positive real component.

3. Dynamical Analysis

This section looks at the chaotic dynamics of the suggested circulant system (Eq. (2)). We analyze Lyapunov exponents, bifurcations, and coexisting attractors.

3.1. *Phase portrait*

The proposed circulant chaotic system has a diverse dynamical behavior, with six coexisting chaotic attractors and four stable equilibrium points. These

Fig. 1. The consistent color-coding scheme employed throughout the paper to separate the dynamics of each attractor and equilibrium point.

chaotic attractors are arranged in two groups of three, each with circulant symmetry. To aid visualization and analysis, a consistent color-coding scheme (shown in Fig. 1) is employed throughout the paper to separate the dynamics of each attractor and equilibrium point.

The four stable equilibrium points, denoted as FP_1 through FP_4, are assigned colors 1–4 in the color-coding scheme. Their coordinates are

$$FP_1 = (0, 0, 0),$$

$$FP_2 = (-0.1516, -0.4819, -0.4819),$$

$$FP_3 = (-0.4819, -0.1516, -0.4819),$$

$$FP_4 = (-0.4819, -0.4819, -0.1516).$$

These equilibrium points correspond to stable regions in the phase space, where trajectories converge for certain initial conditions.

The system also features six chaotic attractors, grouped into two distinct sets based on their initial conditions and symmetry properties. Each set consists of three attractors that are cyclic permutations of one another, reflecting the circulant symmetry of the system. The first group of chaotic attractors

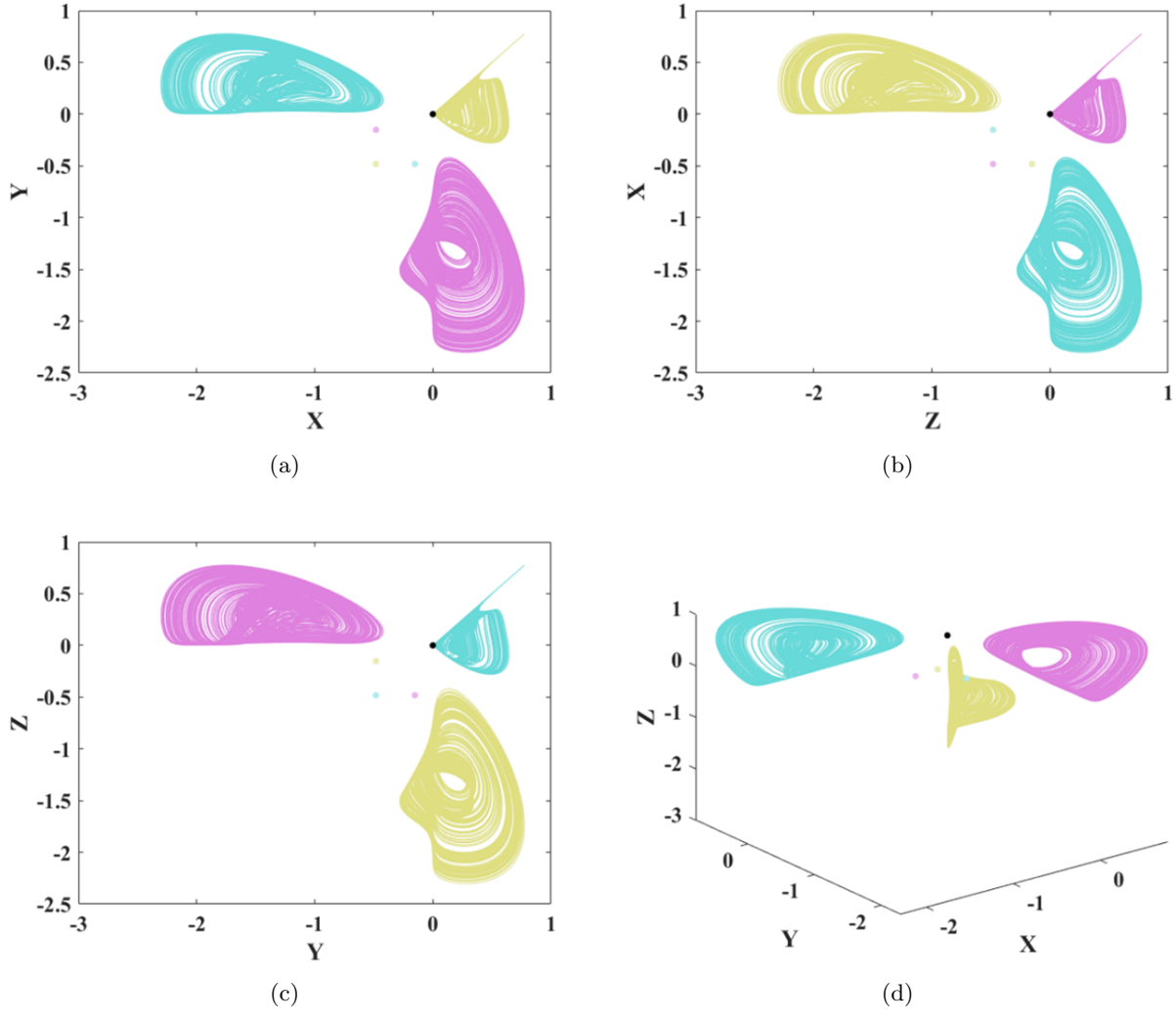

Fig. 2. Four stable equilibria and chaotic dynamics of Eq. (2) correspond to the initial conditions $IC_{05} = (-0.67, 0.92, 0.4)$, $IC_{06} = (0.4, -0.67, 0.92)$, $IC_{07} = (0.92, 0.4, -0.67)$, where colors 5–7 are used to represent the chaotic respective dynamics; the three attractors in (a) X–Y plane, (b) Z–X plane, (c) Y–Z plane and (d) X–Y–Z space.

corresponds to the initial conditions $IC_{05} = (-0.67, 0.92, 0.4)$, $IC_{06} = (0.4, -0.67, 0.92)$, $IC_{07} = (0.92, 0.4, -0.67)$. These attractors are plotted in Fig. 2, where colors 5–7 are used to represent their respective dynamics. The cyclic permutation of initial conditions ensures that the attractors exhibit symmetric behavior in the phase space. The second group of chaotic attractors corresponds to the initial conditions $IC_{08} = (-1.51, -0.275, 0)$, $IC_{09} = (0, -1.51, -0.275)$, $IC_{10} = (-0.275, 0, -1.51)$. These attractors are plotted in Fig. 3, with colors 8–10 distinguishing their dynamics. Similar to the first group, the symmetry of the system ensures that these attractors are cyclic permutations of one another.

The phase portraits in Figs. 2 and 3 highlight the intricate structure of the chaotic attractors, showcasing their circulant symmetry. The coexistence of multiple attractors underscores the multistability of the system, which has potential applications in secure communication, random number generation, and other fields requiring complex dynamical behavior.

3.2. *Bifurcation analysis*

Bifurcation diagrams are computed by adjusting three important parameters (a, b, and c) utilizing various forward and backward continuation techniques in order to investigate the dynamical transitions of the suggested circulant chaotic system. To investigate the dynamics of each attractor by changing each parameter, we plot bifurcation diagrams, starting from $a = -\frac{1}{18}$, $b = -1$, $c = -1$,

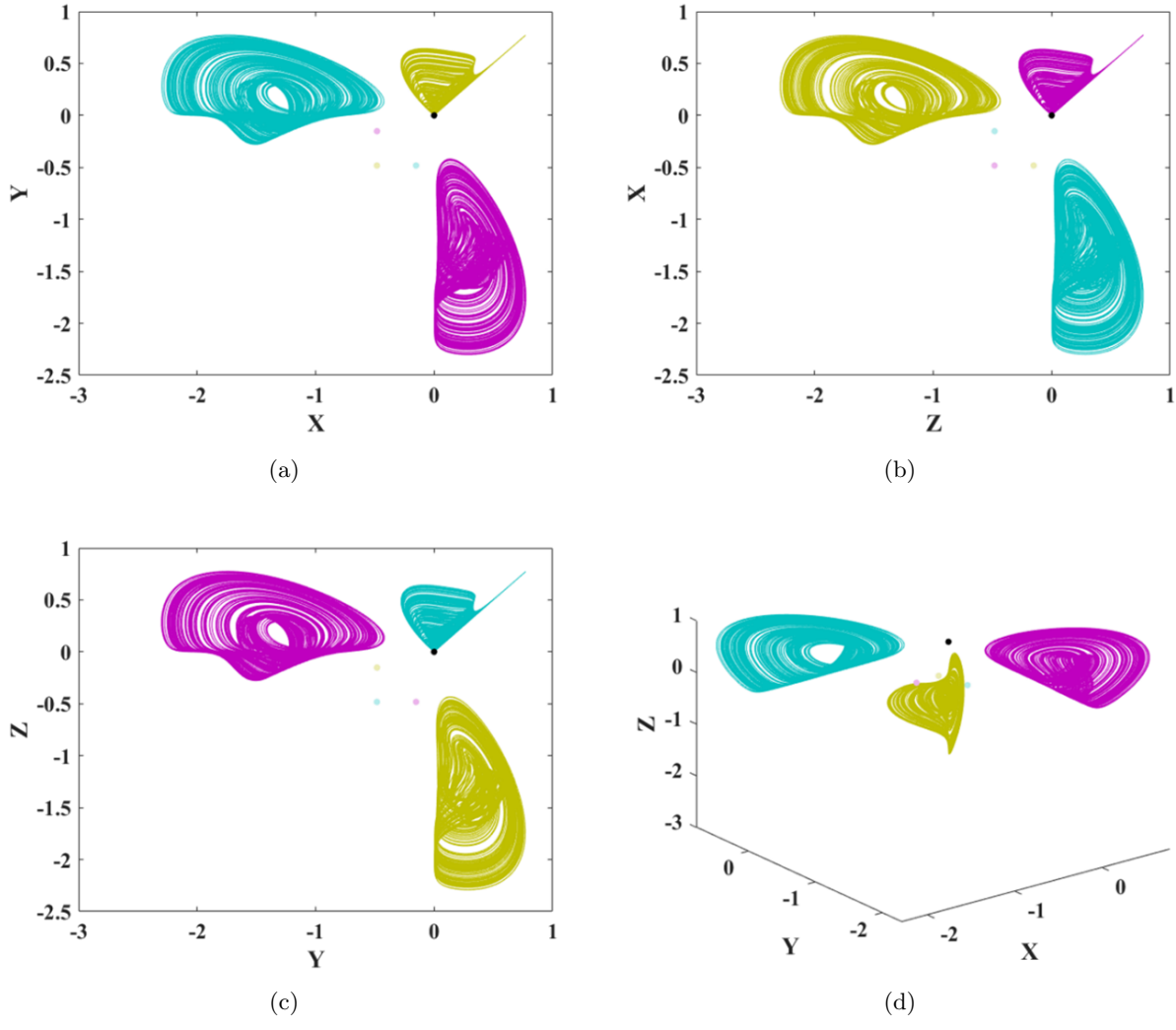

Fig. 3. Four stable equilibria and chaotic dynamics of Eq. (2) correspond to the initial conditions $IC_{08} = (-1.51, -0.275, 0)$, $IC_{09} = (0, -1.51, -0.275)$, $IC_{10} = (-0.275, 0, -1.51)$, with colors 8–10 distinguishing the chaotic dynamics; the three attractors in (a) X–Y plane, (b) Z–X plane, (c) Y–Z plane and (d) X–Y–Z space.

by increasing the bifurcation parameter in a forward method for larger values of the parameter or decreasing the bifurcation parameter in a backward method for smaller values. Then, we chose to plot the bifurcations that have more diverse dynamics. These graphs demonstrate the circulant symmetry of the attractors and show how sensitive the system is to changes in parameters.

Case 1. Varying Parameter a

In the first scenario, the bifurcation diagram by changing the parameter a is investigated. Bifurcation diagrams for the two sets of three chaotic attractors are shown in Figs. 4 and 5 as the parameter a is changed. In each figure, the bifurcations of three attractors of each group are plotted by their corresponding colors. Bifurcation diagrams with the first set of initial conditions IC_{05}, IC_{06}, IC_{07}, and forward continuation are shown in Fig. 4, which presents the circulant symmetry of attractors by varying a. Each panel of the figure shows the bifurcations from the viewpoint of one of the system's variables. Comparing the bifurcations from the viewpoint of various variables also discloses the circulant symmetry of the three attractors of the system. The circulant symmetry can be seen as the bifurcation diagram of the attractor, with color 7 in the $X_{\max}$ plot which is the same as for the attractor with color 5 in the $Y_{\max}$ plot and for the attractor with color 6 in the $Z_{\max}$ plot. Figure 5 shows the bifurcation diagrams of chaotic attractors with IC_{08}, IC_{09}, IC_{10}, and forward continuation by changing a. Since the dynamics for each group are cyclic permutations of each other under the same parameter change, both pictures show the circulant symmetry of the attractors.

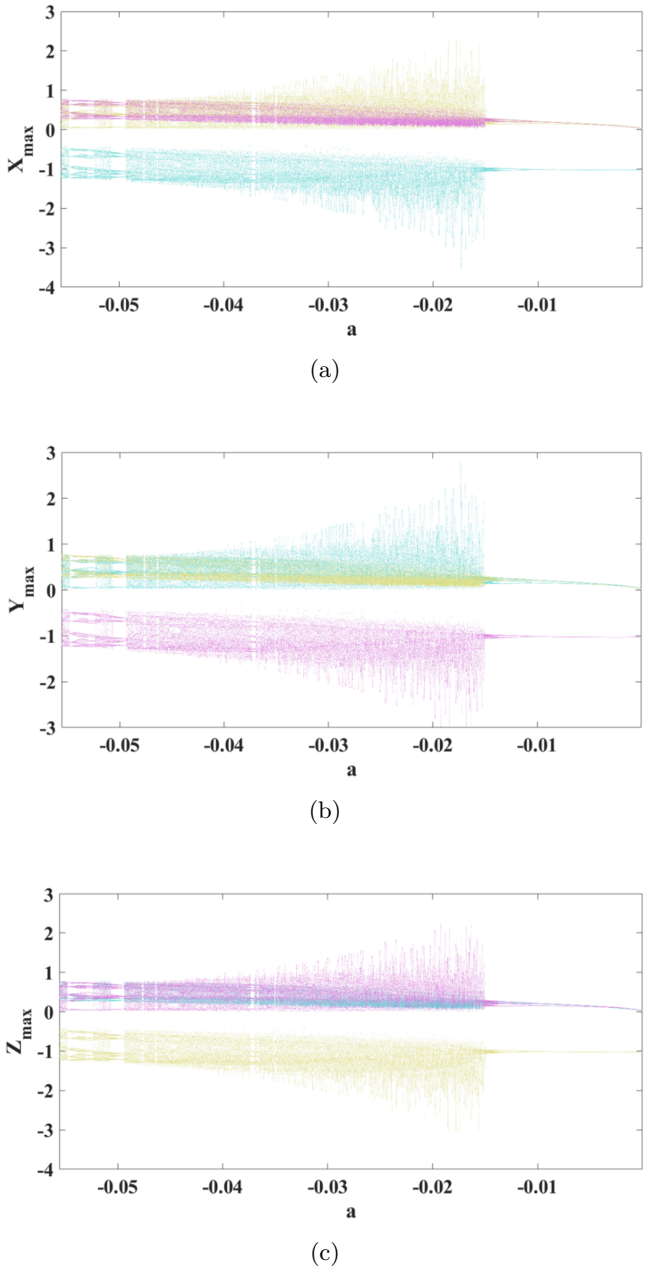

Fig. 4. Bifurcation diagram by changing the parameter a with the first set of initial conditions IC_{05}, IC_{06}, IC_{07}, and forward continuation; the maximum value of (a) X variable, (b) Y variable and (c) Z variable.

Case 2. Varying Parameter b

In the second scenario, the bifurcation diagram by changing the parameter b is investigated. Figures 6 and 7 present bifurcation diagrams obtained using the backward continuation method, where the parameter b is varied. Figure 6 represents the first group of attractors' bifurcations (IC_{05}, IC_{06}, IC_{07}), while Fig. 7 represents the second group of attractors (IC_{08}, IC_{09}, IC_{10}). These diagrams highlight the system's multistability and the influence of parameter b on the coexisting attractors. The backward continuation method reveals discontinuous transitions, providing insights into the system's complex behavior.

Case 3. Varying Parameter c

The third scenario analyzes bifurcations using varying parameters c. Bifurcation diagrams produced by the forward continuation approach, where the parameter c is changed, are shown in Figs. 8 and 9. Figure 8 identifies the first group of attractors (IC_{05}, IC_{06}, IC_{07}), and Fig. 9 identifies the second group of attractors (IC_{08}, IC_{09}, IC_{10}). By displaying routes to chaos (such as period-doubling cascades) and

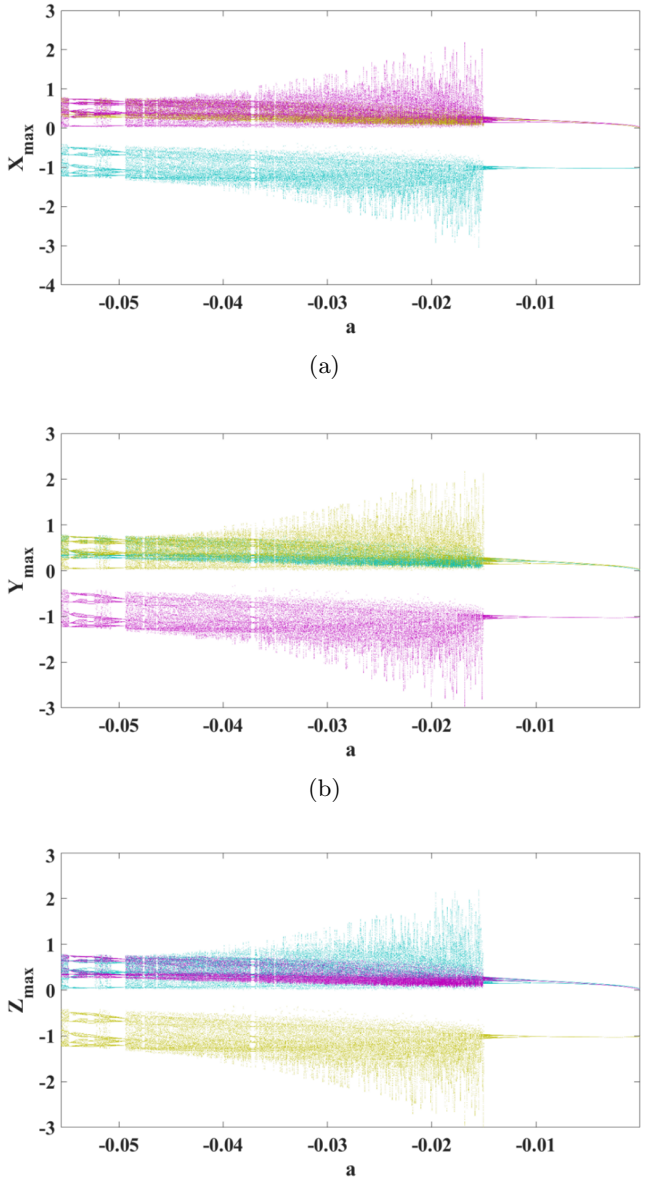

Fig. 5. Bifurcation diagram by changing the parameter a with the second set of initial conditions IC_{08}, IC_{09}, IC_{10} and forward continuation; the maximum value of (a) X variable, (b) Y variable and (c) Z variable.

the continuity of circulant symmetry across parameter changes, these diagrams point out the system's dependence on parameter c.

Bifurcation diagrams draw attention to the system's fundamental characteristics. The system's circulant symmetry is visible in every situation. Because the governing equations are inherently symmetric, the dynamics for each group of attractors are cyclic permutations of each other. Different dynamical behaviors emerge from varied initial conditions, confirming the coexistence of attractors. Random number generation and secure communication are two possible uses for this characteristic. Rich dynamical transitions are present in the system, such as periodic windows, chaotic regions, and abrupt changes. These changes highlight the intricacy of the system and its potential for real-world uses.

3.3. *Lyapunov spectrum*

We examine the circulant system's Lyapunov spectrum, a crucial property for comprehending the

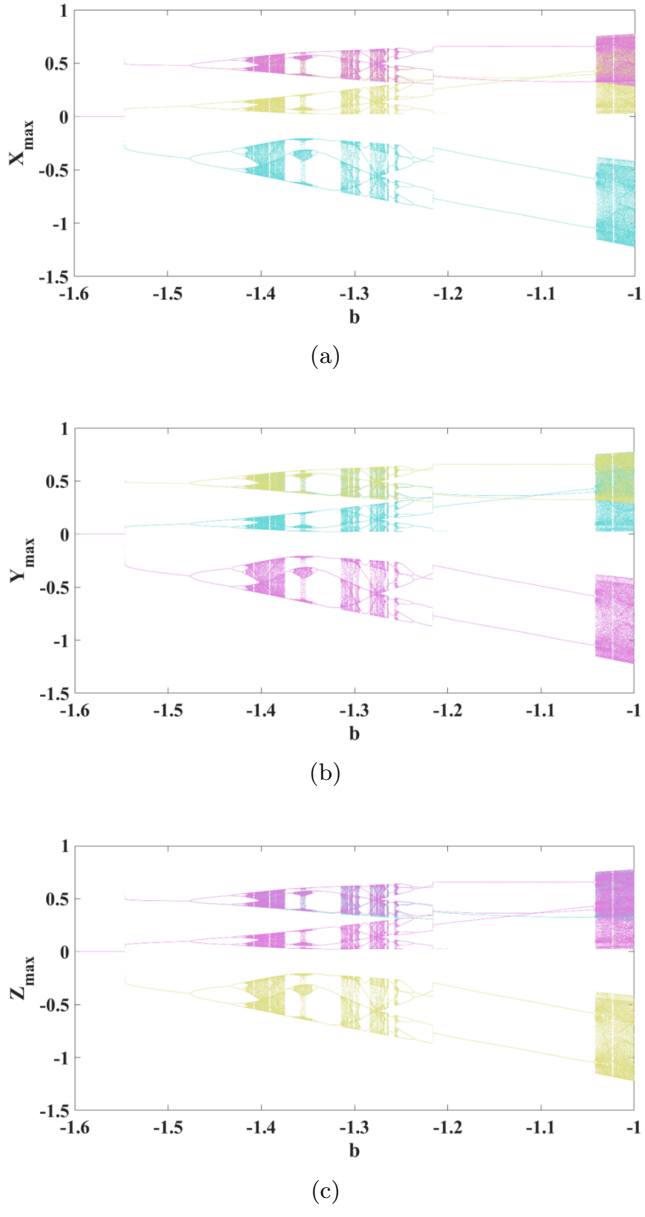

Fig. 6. Bifurcation diagram by changing the parameter b with the first set of initial conditions IC_{05}, IC_{06}, IC_{07} and backward continuation; the maximum value of (a) X variable, (b) Y variable and (c) Z variable.

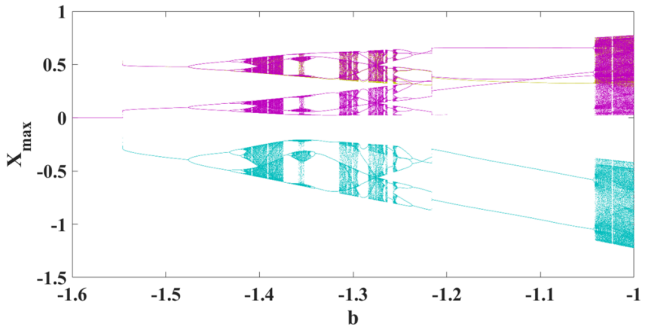

(a)

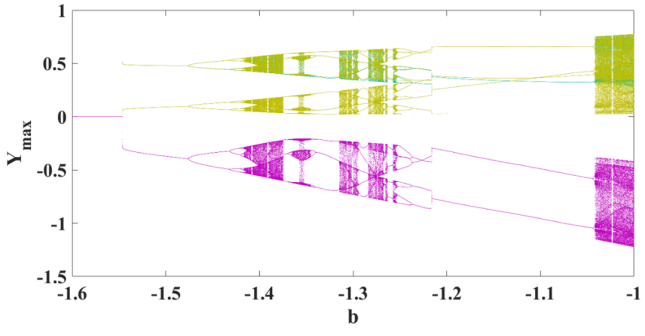

(b)

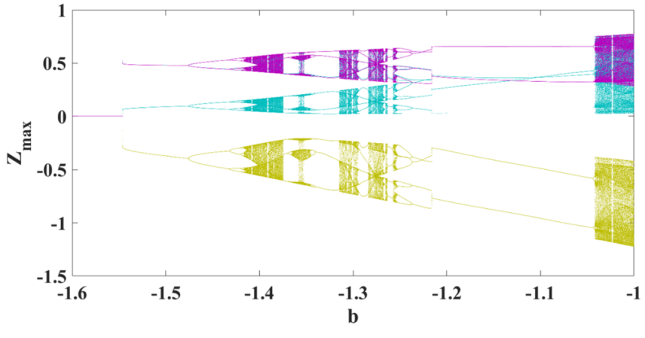

(c)

Fig. 7. Bifurcation diagram by changing the parameter b with the second set of initial conditions IC_{08}, IC_{09}, IC_{10} and backward continuation; the maximum value of (a) X variable, (b) Y variable and (c) Z variable.

stability and complexity of dynamical systems, in order to learn more about its chaotic dynamics. The Lyapunov exponents, which provide important information about periodicity, chaos, and bifurcation points, quantify the exponential divergence or convergence rates of neighboring trajectories in phase space. They are computed with the Wolf method [Wolf *et al.*, 1985] and runtime 20 000. Here, parameters a, b, and c are systematically changed to concentrate on the dynamic variations. Each set of three attractors has the same dynamics because of the system's circulant symmetry. Therefore, we examine the Lyapunov spectra of one typical attractor from each group (for example, the attractors that correspond to colors 5 and 8).

Case 1. Varying Parameter a

The Lyapunov spectra of the attractors corresponding to colors 5 and 8 are shown in Figs. 10(a) and 10(b) as parameter a is changed. Notably, the two attractors exhibit identical dynamics and Lyapunov exponents, consistent with the circulant

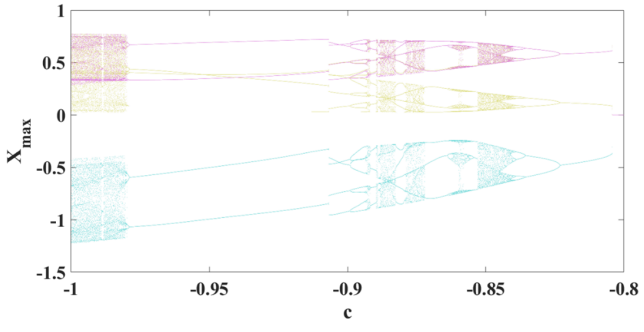

(a)

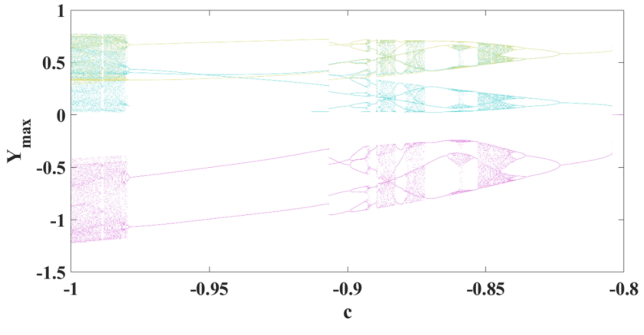

(b)

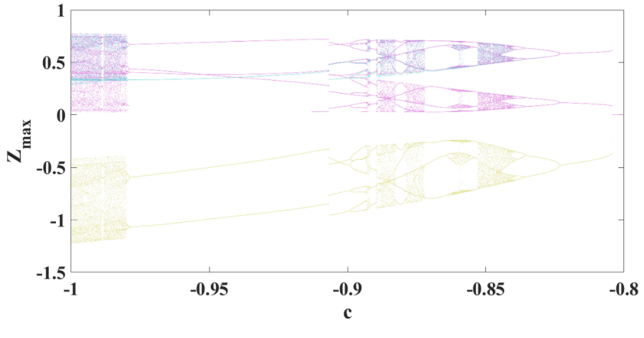

(c)

Fig. 8. Bifurcation diagram by changing the parameter c with the first set of initial conditions IC_{05}, IC_{06}, IC_{07}, and forward continuation; the maximum value of (a) X variable, (b) Y variable and (c) Z variable.

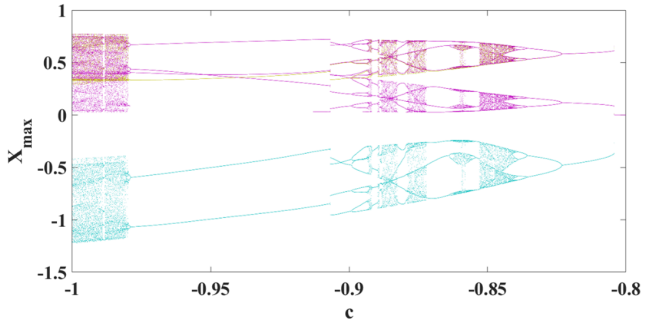

(a)

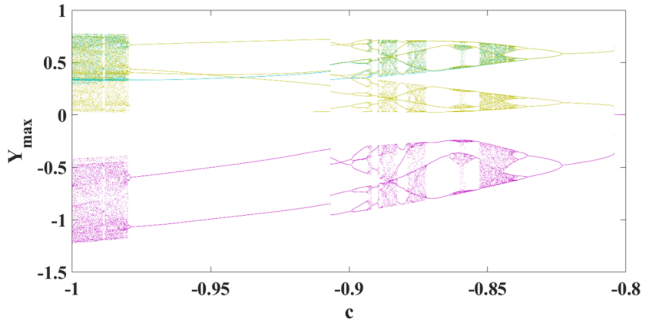

(b)

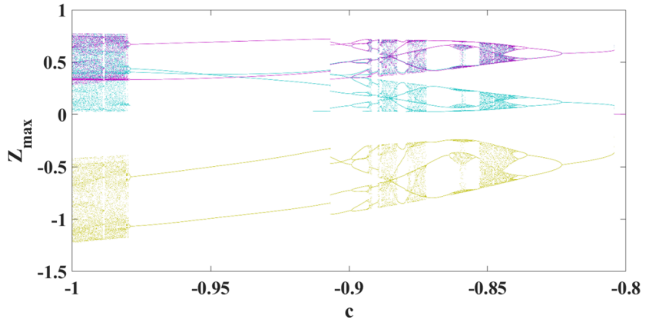

(c)

Fig. 9. Bifurcation diagram by changing the parameter c with the second set of initial conditions IC_{08}, IC_{09}, IC_{10}, and forward continuation; the maximum value of (a) X variable, (b) Y variable and (c) Z variable.

symmetry of the system. For small a, the system exhibits periodic windows (among the chaotic dynamics), characterized by all Lyapunov exponents being nonpositive. By intermediate a, a large chaotic attractor emerges as a result of a crisis. This transition is marked by the appearance of a positive Lyapunov exponent, indicating sensitive dependence on initial conditions. In large a, the chaotic attractor contracts after another crisis, and then there is an inverse period-doubling route to chaos. Also, the Lyapunov spectrum reflects the bifurcation points, with one exponent going toward zero and then returning. The dynamical variation is confirmed by the Lyapunov spectrum. Chaos is shown by one positive Lyapunov exponent, periodicity by one zero Lyapunov exponent and the rest negative, and equilibrium as all Lyapunov exponents are negative.

Case 2. Varying Parameter b

The Lyapunov spectra of the colors 5 and 8 attractors as parameter b is changed are shown in Fig. 11. Throughout the parameter range, the dynamics experience notable changes. In small b, all Lyapunov exponents are negative, indicating that the attractor corresponds to a stable equilibrium point. By intermediating b, a jump to a limit cycle occurs, marked by one zero Lyapunov exponent and the rest negative. Then, chaos, which is defined by one positive Lyapunov exponent, is followed by a period-doubling cascade. In large b, complex interactions between attractors are reflected in the system's alternating chaotic and periodic windows. A crisis eventually leads to a larger chaotic attractor.

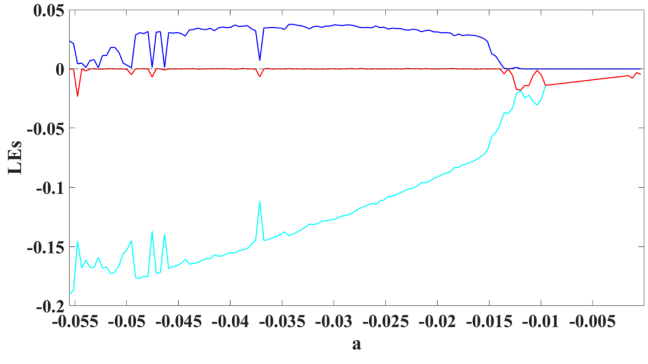

(a)

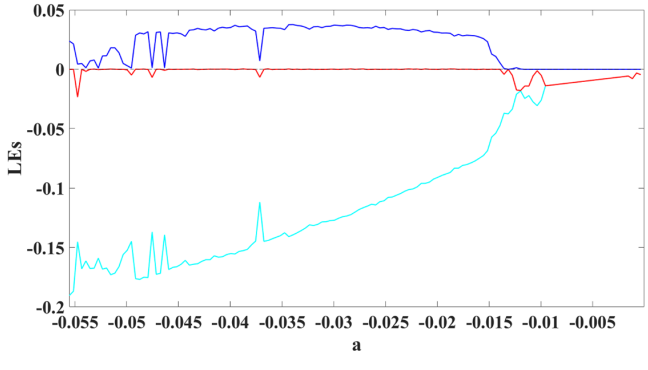

(b)

Fig. 10. The Lyapunov spectra of the attractors corresponding to colors (a) 5 and (b) 8 as parameter a is changed.

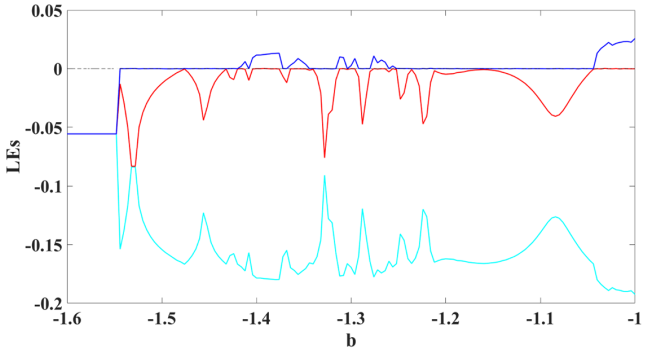

(a)

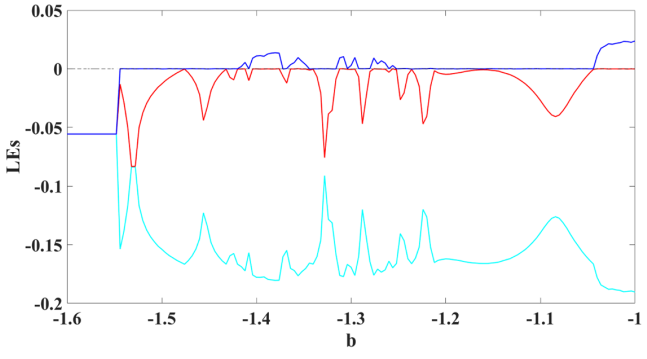

(b)

Fig. 11. The Lyapunov spectra of the attractors corresponding to colors (a) 5 and (b) 8 as parameter b is changed.

These transitions are highlighted by the Lyapunov exponents in Fig. 11. Stable equilibrium is observed when there are three negative exponents, limit cycle by one zero exponent and two negative exponents, and chaos by one positive exponent, one zero exponent, and one negative exponent. When at least one Lyapunov exponent goes to zero, it indicates a regime change.

Case 3. Varying Parameter c

As parameter c changes, the Lyapunov spectra for the identical attractors (colors 5 and 8) are displayed in Fig. 12. There are rich transitions in the dynamics. For small c, there is only one positive Lyapunov exponent, indicating that the system is chaotic. In intermediate c, the dynamics shift to a limit cycle, where the highest Lyapunov exponent drops to zero. For large c, periodic and chaotic windows alternate, followed by an inverse period-doubling route to chaos. Eventually, the dynamics collapse to a stable equilibrium point via a sudden transition from a limit cycle. The transitions which are captured by the Lyapunov spectrum in Fig. 12 are chaos when one exponent is positive, limit cycle when there are two negative exponents and one zero exponent, and equilibrium when all exponents are negative.

3.4. *Basin of attraction*

The basins of attraction provide significant insight into the system's multistability by illustrating how initial conditions influence which attractor a trajectory converges to. To depict these basins, we examine the circulant chaotic system in three orthogonal planes: x_0–y_0 (when $z_0 = 0$), y_0–z_0 (when $x_0 = 0$), and z_0–x_0 (when $y_0 = 0$). The results are shown in Fig. 13. Each color corresponds to one of the ten coexisting attractors identified earlier in the investigation. We use a consistent color scheme to make interpretation easier.

Several intriguing features emerge from the basins of attraction, highlighting the unique dynamical properties of the circulant chaotic system. One particularly noteworthy characteristic is the V-shaped boundaries observed in the basins. Such geometric patterns are extremely rare in the basins of conventional dynamical systems and reflect a

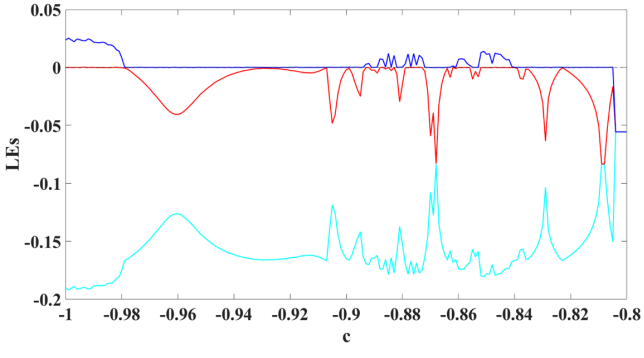

(a)

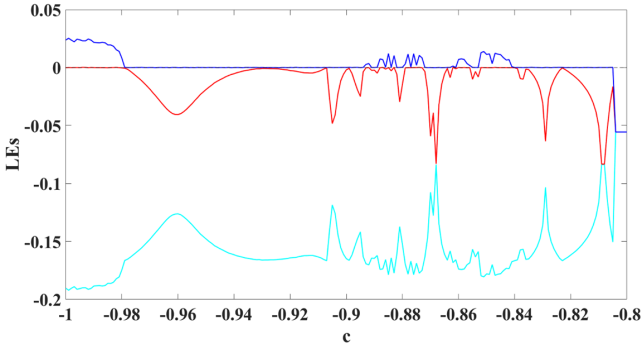

(b)

Fig. 12. The Lyapunov spectra of the attractors corresponding to colors (a) 5 and (b) 8 as parameter c is changed.

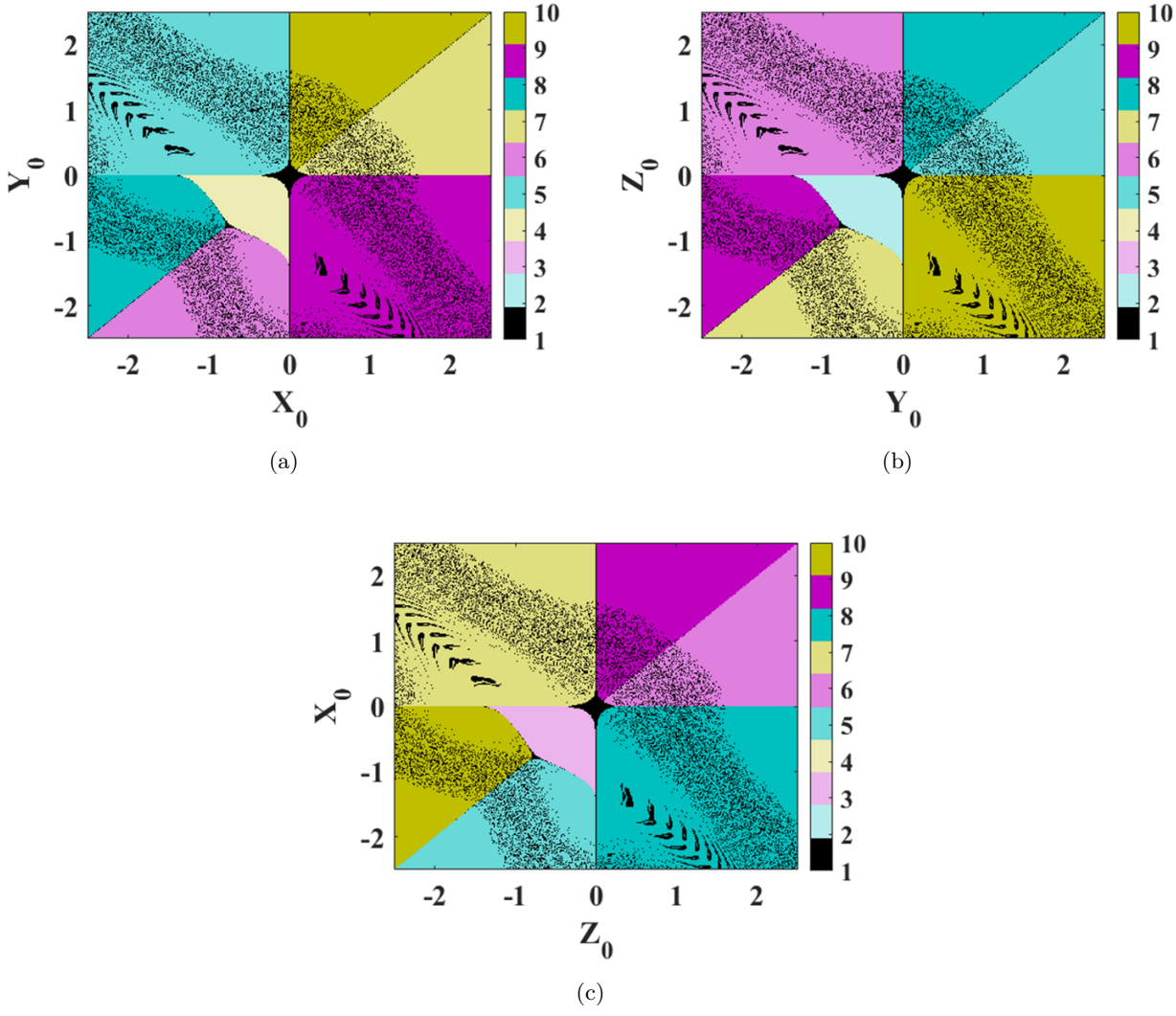

Fig. 13. The basins of attraction for the circulant chaotic system in three orthogonal planes; (a) in x_0–y_0 (when $z_0 = 0$), (b) in y_0–z_0 (when $x_0 = 0$) and (c) in z_0–x_0 (when $y_0 = 0$).

particular interplay between attractors. These V-shaped borders presumably develop due to the nonlinear interactions in the system's governing equations, which create sharp transitions between regions dominated by various attractors.

Another striking feature is the basin associated with the stable equilibrium at the origin. Unlike the other attractors, whose basins occupy contiguous regions in phase space, the basin of the origin appears as a "powder-like" distribution scattered throughout the basins of the other attractors. This fragmented structure implies that trajectories are particularly susceptible to perturbations, as they can be dragged into the origin depending on minor alterations in initial conditions. This phenomenon represents the delicate balance between stability and chaos in the system.

When comparing the three basin plots in Fig. 13 (corresponding to the x_0–y_0, y_0–z_0, and z_0–x_0 planes), the same patterns are obvious, underlining the circulant symmetry of the system. Consistent geometric shapes across all planes demonstrate that the system's dynamics are invariant by cyclic permutations of variables.

4. Conclusion

In this study, we introduced a novel Three-Dimensional (3D)-chaotic flow characterized by circulant symmetry. The system exhibits rich and complex dynamical behavior, including dissipative dynamics over the studied parameter range. A detailed equilibrium analysis revealed that four of the fifteen fixed points within the system are stable.

Notably, the system supports two distinct sets of three coexisting chaotic attractors, each maintaining the system's underlying circulant symmetry, making it the first reported chaotic system with such properties to the best of our knowledge.

Bifurcation diagrams concerning all three system parameters illustrated the wide range of dynamical regimes, from periodic to chaotic behavior, which was further confirmed by computing the corresponding Lyapunov exponent spectra. The basins of attraction exhibited unusual V-shaped boundaries, highlighting the complexity of the system's multistability. Moreover, the circulant symmetry was visually evident in the basin structures when projected onto the three orthogonal planes.

These findings not only expand the current understanding of symmetric chaotic systems but also open new directions for exploring complex dynamics in systems with structured symmetry. Future work may include investigating potential applications in secure communication, random number generation, or synchronization phenomena based on this unique chaotic flow.

Author's Contributions

Karthikeyan Rajagopal: Conceptualization, Investigation, Writing — original draft,

Fahimeh Nazarimehr: Conceptualization, Methodology, Writing — original draft,

Sajad Jafari: Methodology, Validation, Writing — review and editing,

Julien C. Sprott: Software, Supervision, Writing — review and editing.

Conflict of Interest

The authors declare that they have no conflict of interest.

Data Availability

Data generated during this study will be made available on reasonable request.

ORCID

Karthikeyan Rajagopal
https://orcid.org/0000-0003-2993-7182
Fahimeh Nazarimehr
https://orcid.org/0000-0002-2664-9006
Sajad Jafari
https://orcid.org/0000-0002-6845-7539
Julien C. Sprott
https://orcid.org/0000-0001-7014-3283

References

Almatroud, O. A., Shukur, A. A., Pham, V.-T. & Grassi, G. [2024] "Oscillator with line of equilibiria and nonlinear function terms: Stability analysis, chaos, and application for secure communications," *Mathematics* **12**, 1874.

Banerjee, S. [2010] *Chaos Synchronization and Cryptography for Secure Communications*: *Applications for Encryption* (IGI Global).

Bob, P. [2007] "Chaos, brain and divided consciousness," *Acta Univ. Carol. Med. Monogr.* **153**, 9–80.

Danca, M.-F. [2017] "Hidden chaotic attractors in fractional-order systems," *Nonlin. Dyn.* **89**, 577–586.

Danca, M.-F. [2024] "Chaotic hidden attractor in a fractional order system modeling the interaction between dark matter and dark energy," *Commun. Nonlin. Sci. Numer. Simul.* **131**, 107838.

Khan, A., Li, C., Zhang, X. & Cen, X. [2025] "A two-memristor-based chaotic system with symmetric bifurcation and multistability," *Chaos Fract.* **2**, 1–7.

Kyurkchiev, N., Zaevski, T., Iliev, A., Kyurkchiev, V. & Rahnev, A. [2024] "Generating chaos in dynamical systems: Applications, symmetry results, and stimulating examples," *Symmetry* **16**, 938.

Lawnik, M., Moysis, L. & Volos, C. [2022] "Chaos-based cryptography: Text encryption using image algorithms," *Electronics* **11**, 3156.

Li, C. & Sprott, J. C. [2021] "Multi-stability in symmetric systems," in *Chaotic Systems with Multistability and Hidden Attractors* (Springer International Publishing), pp. 311–329.

Li, C., Sprott, J. C., Zhang, X., Chai, L. & Liu, Z. [2022] "Constructing conditional symmetry in symmetric chaotic systems," *Chaos Solit. Fract.* **155**, 111723.

Nazarimehr, F. & Sprott, J. C. [2020] "Investigating chaotic attractor of the simplest chaotic system with a line of equilibria," *Eur. Phys. J. Spec. Top.* **229**, 1289–1297.

Pan, G., Li, C., Liu, W., Xue, Y. & Qi, X. [2025] "Countless coexisting chaotic attractors: From system construction to FPGA-based observation," *Chaos Solit. Fract.* **198**, 116610.

Panahi, S., Shirzadian, T., Jalili, M. & Jafari, S. [2019] "A new chaotic network model for epilepsy," *Appl. Math. Comput.* **346**, 395–407.

Panahi, S., Nazarimehr, F., Jafari, S., Sprott, J. C., Perc, M. & Repnik, R. [2021] "Optimal synchronization of circulant and non-circulant oscillators," *Appl. Math. Comput.* **394**, 125830.

Rajagopal, K., Akgul, A., Pham, V.-T., Alsaadi, F. E., Nazarimehr, F., Alsaadi, F. E. & Jafari, S. [2019] "Multistability and coexisting attractors in a new circulant chaotic system," *Int. J. Bifurcation and Chaos* **29**, 1950174.

Raza, N., Amjad, Z., Rani, B., Almalki, Y. & Bayram, M. [2025] "Exploring chaos, multistability, and interaction patterns in (3 + 1)-dimensional KdV-BBM model," *Nonlin. Dyn.* **113**, 11969–11986.

Rössler, O. [1976] "An equation for continuous chaos," *Phys. Lett. A* **57**, 397–398.

Shukur, A. A., Neamah, A. A., Pham, V.-T. & Grassi, G. [2025] "A novel chaotic system with one absolute term: Stability, ultimate boundedness, and image encryption," *Heliyon* **11**, e37239.

Sprott, J. C. [2010] *Elegant Chaos*: *Algebraically Simple Chaotic Flows* (World Scientific).

Tutueva, A., Nepomuceno, E. G., Moysis, L., Volos, C. & Butusov, D. [2022] "Adaptive chaotic maps in cryptography applications," in *Cybersecurity* (Springer International Publishing), pp. 193–205.

Wang, X. & Chen, G. [2012] "A chaotic system with only one stable equilibrium," *Commun. Nonlin. Sci. Numer. Simul.* **17**, 1264–1272.

Wang, N., Cui, M., Yu, X., Shan, Y. & Xu, Q. [2024] "Generation of no-equilibrium multi-fold chaotic attractor for image processing and security," *Appl. Math. Model.* **133**, 271–285.

Wei, Z. [2011] "Dynamical behaviors of a chaotic system with no equilibria," *Phys. Lett. A* **376**, 102–108.

Wolf, A., Swift, J. B., Swinney, H. L. & Vastano, J. A. [1985] "Determining Lyapunov exponents from a time series," *Physica D* **16**, 285–317.

Xu, Q., Tan, X., Zhu, D., Bao, H., Hu, Y. & Bao, B. [2020] "Bifurcations to bursting and spiking in the Chay neuron and their validation in a digital circuit," *Chaos Solit. Fract.* **141**, 110353.

Xu, Q., Wang, K., Chen, M., Parastesh, F. & Wang, N. [2024a] "Bursting and spiking activities in a Wilson neuron circuit with memristive sodium and potassium ion channels," *Chaos Solit. Fract.* **181**, 114654.

Xu, Q., Wang, K., Shan, Y., Wu, H., Chen, M. & Wang, N. [2024b] "Dynamical effects of memristive electromagnetic induction on a 2D Wilson neuron model," *Cogn. Neurodyn.* **18**, 645–657.

Zhang, X., Li, C., Lei, T., Iu, H. H.-C. & Kapitaniak, T. [2025] "Coexisting hyperchaos in a memristive neuromorphic oscillator," *IEEE Trans. Comput.-Aided Des. Integr. Circuits Syst.* **44**, 3179–3188.